Nonlinear resonances in magnetic and frequency scanning systems of three-level Λ- and V-systems

Yu.V. Bogdanova

Institute of Atmospheric Optics,
Siberian Branch of the Russian Academy of Sciences, Tomsk

Received March 28, 2003

To model signals of magnetic and frequency scanning of a rarefied gas, the problem of resonant interaction of two counterrunning monochromatic waves and particles with the active transition $J = 0 \leftrightarrow J = 1$ in a stationary magnetic field is solved in semi-classical approximation by the method of density matrix. A resonance with the sign depending on the gas pressure, wave intensity, and magnetic field is found for systems with a split ground state.

Introduction

It is well known that interference of neighboring transitions can significantly deform the shape of a resonance fluorescence line[1] and even completely suppress absorption.[2] The degree of realization of quantum interference effects resonantly depends on the medium and radiation parameters. Therefore, we can assume that, matching the model, frequency, and intensity of laser radiation and achieving maximal interference parameters of the line shape, it is possible to reconstruct with high accuracy the medium or radiation characteristics from spectroscopic data.

The best analog to the proposed method is the method of level overlapping based on the dependence of interference on the split between sublevels. From the magnetic scanning signal, the atomic constant and interaction constants are determined or the inverse problem is solved: with known medium parameters the external magnetic field is measured.[3]

In the case of the classic level overlapping method, the scanning signal is assumed to depend linearly on weak intensity of the incident radiation. The current progress in scientific instrumentation allows studying magnetic scanning signals and analyzing nonlinear effects at high pumping power. The nonlinear Faraday effect in helium was studied experimentally in Ref. 4. It was noted that the existing theories well agree with the experiment only for nonsaturated absorption, but fail to predict the medium translucence in a zero magnetic field, which is observed experimentally at strong fields.

Spectroscopic nonlinear resonances can be observed at close-to-saturation intensities. To separate resonances in the Doppler profile, the pump-probe technique or velocity-selective optical pumping are commonly used.[5] For example, the absorption line of a weak wave in neon excited by a high-power counter running wave looks like a narrow resonance against the background of a wide Doppler signal,[6] and the pump power augmentation leads to the resonance broadening and splitting.

This paper presents analytical and numerical analysis of resonance fluorescence spectra and magnetic scanning signals for an ensemble of three-level systems with the magnetically split upper or lower levels in the field of counterpropagating waves of an arbitrary intensity.

1. Problem formulation and general solution

Assume that a cell with atoms or molecules of a rarefied gas is in a constant magnetic field H directed along the axis z. Monochromatic traveling waves, polarized along the axis x, with the frequencies $\omega_\pm$ and amplitudes $E_\pm$ propagate in the opposing direction along the axis y:

$$E = E_- \cos(\omega_- t - k_- y) +$$

$$+ E_+ \cos(\omega_+ t + k_+ y + \varphi),$$

where t is the time; $k_\pm$ are wave vectors of the corresponding waves; φ is the phase shift. In the case of equal amplitudes and frequencies, the traveling waves form a standing wave.

Assume that the wave frequencies are resonant to transitions between the ground and excited states of a gas particle, and for the Λ-system the angular momentum of the ground state is 1 and that of the excited state is 0, while for the V-system the angular momentum of the ground state is 0 and that of the excited state is 1. The constant magnetic field splits the state with c $J = 1$ into three sublevels m equal to 0 and ±1 denoted from here on as the 0th, 1st, and 2nd sublevels, respectively. In the assumed experimental geometry, the optical radiation activates transitions with $\Delta m = \pm 1$. Further we treat gas atoms or molecules as three-level Λ-systems, assuming the transitions between the upper and two lower sublevels to be allowed with the dipole moment d and the transition between the lower levels to be forbidden with the zero dipole moment or as V-systems with the same

0235-6880/03/07 521-09 $02.00

dipole moment of transitions from the ground state into the split excited one.

Introduce the following designations: omit the second subscript in diagonal elements of the density matrix and represent the off-diagonal elements of the density matrix as sums of two terms proportional to the fast oscillating periodic component

$$\rho_{jj} = \rho_j,\ (j = 1,2,3);\ \rho_{21} = r;$$

$$\rho_{31} = R_{1-}e^{-i(\omega_- t - k_- y)} + R_{1+}e^{-i(\omega_+ t + k_+ y + \varphi)},$$

$$\rho_{32} = R_{2-}e^{-i(\omega_- t - k_- y)} + R_{2+}e^{-i(\omega_+ t + k_+ y + \varphi)}.$$

The steady-state equations for elements of the density matrix of the symmetric Λ-system (the allowed transitions have the equal rates of spontaneous decay $A_1 = A_2 = A$ and broadening constants $\Gamma_1 = \Gamma_2 = \Gamma$; the broadening constant of the forbidden transition is Γ_3) in the standard approximations of a rotating wave, uniform broadening of a line profile, interaction representation, and in the model of relaxation constants[7] with the above designations have the form:

$$\begin{aligned}
A\rho_3 + \gamma(\rho_2 - \rho_1) &= 2\mathrm{Im}(V_-R_{1-} + V_+R_{1+}),\\
A\rho_3 - \gamma(\rho_2 - \rho_1) &= 2\mathrm{Im}(V_-R_{2-} + V_+R_{2+});\\
(\delta_{1-} - i\Gamma)R_{1-} &= V_-(r + \rho_1 - \rho_3),\\
(-\delta_{1+} - i\Gamma)R_{1+} &= V_+(r + \rho_1 - \rho_3),\\
(\delta_{2-} - i\Gamma)R_{2-} &= V_-\left(r^* + \rho_2 - \rho_3\right),\\
(-\delta_{2+} - i\Gamma)R_{2+} &= V_+\left(r^* + \rho_2 - \rho_3\right);\\
(2\Delta - i\Gamma_3)r &= V_-\left(R_{1-} - R_{2-}^*\right) + V_+\left(R_{1+} - R_{2+}^*\right),
\end{aligned} \tag{1}$$

where * denotes the complex conjugation; γ is the collisional relaxation constant; $2\Delta = 2g\mu_0 H/\hbar$ is the split of the lower state; g is the Lande factor; μ_0 is the Bohr magneton, $V_\pm$ is the Rabi frequency of the corresponding wave. Since the solution depends on the square Rabi frequency, below we use the parameter $W_\pm = V_\pm^2$ proportional to the intensity of the traveling wave $I_\pm$. In CGSE units, we have

$$W_\pm = \left(dE_\pm/2\hbar\right)^2 = \frac{d^2}{4\hbar^2}\frac{8\pi I_\pm}{c} = \frac{2\pi d^2}{c\hbar^2}I_\pm.$$

The frequency shifts δ_j depend on the split magnitude, resonance accuracy, and the velocity of a particular particle:

$$\delta_{1-} = k_-v + \Omega_- + \Delta;\ \delta_{1+} = -k_+v + \Omega_+ + \Delta,$$

$$\delta_{2-} = -k_-v - \Omega_- + \Delta;\ \delta_{2+} = k_+v - \Omega_+ + \Delta,$$

where $\Omega_\pm = \omega_{30} - \omega_\pm$ is the frequency detuning of the corresponding traveling wave from the natural frequency of the nonsplit transition ω_{30}; v is the velocity of the particle interacting with the radiation.

The normalization condition for the density matrix

$$\rho_1 + \rho_2 + \rho_3 \equiv F(v)$$

includes the function $F(v)$ determining the density of the velocity distribution of particles in the ensemble in the absence of external effects. This function will be assumed Maxwellian[5]:

$$F(v) = \exp\left(-v^2/\overline{v}^2\right)\Big/\left(\sqrt{\pi}\overline{v}\right),\ \ \overline{v}^2 = 2k_BT/m_a,$$

where $\overline{v}$ is the root-mean-square velocity of particles depending on the Boltzmann constant k_B, the ensemble temperature T, and the particle mass m_a.

Solution of problem (1) for the level populations can be represented as

$$\rho_2^\Lambda(v) = F(v)\left[3 - \frac{A(w + 2q_1 - q_2)}{A(w + q_1) + w(q_1 + q_2) + 2q_1q_2}\right]^{-1},$$

$$\rho_3^\Lambda(v) = F(v)\left[3 + \frac{A(2w + q_1 + q_2)}{w(q_1 + q_2) + 2q_1q_2}\right]^{-1},$$

$$\rho_j = \int_{-\infty}^{+\infty}\rho_j(v)\mathrm{d}v,\ \ j = 1 - 3, \tag{2}$$

where

$$q_1 = \mathrm{Im}\left[(\zeta_{1-} + \zeta_{1+})\vartheta\varsigma\right];\ \ q_2 = \mathrm{Im}\left[(\zeta_{2-} + \zeta_{2+})\vartheta\varsigma\right];$$

$$w = 2\mathrm{Im}\left[(\zeta_{1-} + \zeta_{1+})(\zeta_{2-} + \zeta_{2+})\vartheta\right] + \gamma;$$

$$\vartheta = (\varsigma + s)^{-1};\ \ \varsigma = i\Gamma_3 - 2\Delta;\ \ s = \zeta_{1-} + \zeta_{1+} + \zeta_{2-} + \zeta_{2+}; \tag{3}$$

$$\zeta_{1-} = \frac{W_-}{-i\Gamma + \delta_{1-}};\ \ \zeta_{1+} = \frac{W_+}{-i\Gamma + \delta_{1+}};$$

$$\zeta_{2-} = \frac{W_-}{-i\Gamma + \delta_{2-}};\ \ \zeta_{2+} = \frac{W_+}{-i\Gamma + \delta_{2+}}.$$

The total work of the fields P is proportional to the upper-level population and the sum of the Einstein coefficients of the allowed transitions:

$$\mathrm{P}^\Lambda = 2V_-\,\mathrm{Im}(R_{1-} + R_{2-}) + 2V_+\,\mathrm{Im}(R_{1+} + R_{2+}) = 2A\rho_3^\Lambda, \tag{4}$$

the work of the field of one wave depends on all populations:

$$\mathrm{P}_\pm^\Lambda(v) = -2\mathrm{Im}\left[\left(\Theta^\Lambda - \rho_2^\Lambda\right)\zeta_{2\pm} + \left(\Theta - \rho_1^\Lambda\right)\zeta_{1\pm}\right],$$

$$\mathrm{P}_\pm = \int_{-\infty}^{+\infty}\mathrm{P}_\pm(v)\mathrm{d}v, \tag{5}$$

where $\Theta^\Lambda = \left[(\zeta_{1-} + \zeta_{1+})\rho_1^\Lambda + (\zeta_{2-} + \zeta_{2+})\rho_2^\Lambda + \varsigma\rho_3^\Lambda\right]\vartheta$.

Since $\zeta_{j\pm}$ are proportional to the square Rabi frequency, the work of the field is directly proportional to $W_\pm$, that is, the wave intensity.

For the similar case of the V-system in designations (3) we obtain

$$\rho_2^{\mathrm{V}}(v) = F(v)\left[3 + \frac{A(2w - 2q_2 + 4q_1 + A)}{2\big(w(q_1 + q_2) + 2q_1q_2 + Aq_2\big)}\right]^{-1},$$

$$\rho_3^{\mathrm{V}}(v) = F(v)\left[3 + \frac{A(2\ \ w + 4q_2 - 2q_1 + A)}{2\big(w(q_1 + q_2) + 2q_1q_2 + Aq_1\big)}\right]^{-1},$$

$$\mathrm{P}^{\mathrm{V}} = 2V_-\,\mathrm{Im}(R_{1-} + R_{2-}) +$$

$$+2V_+\,\mathrm{Im}(R_{1+} + R_{2+}) = A\big(\rho_2^{\mathrm{V}} + \rho_3^{\mathrm{V}}\big), \qquad (6)$$

$$\mathrm{P}_\pm^{\mathrm{V}}(v) = 2\mathrm{Im}\Big[\big(\Theta^{\mathrm{V}} - \rho_2^{\mathrm{V}}\big)\zeta_{2\pm} + \big(\Theta - \rho_3^{\mathrm{V}}\big)\zeta_{1\pm}\Big],$$

where $\Theta^{\mathrm{V}} = \big(\varsigma\rho_1^{\mathrm{V}} + (\zeta_{2-} + \zeta_{2+})\rho_2^{\mathrm{V}} + (\zeta_{1-} + \zeta_{1+})\rho_3^{\mathrm{V}}\big)\vartheta$. Note that for the V-system the total work is proportional to the sum of the upper-level populations.

The equations obtained cannot be integrated as they are. The dependence of the work and system population on the velocities of the particles in an ensemble is of independent interest, and, therefore, Section 2 considers the velocity distribution of populations; in Section 3 we present integration, as well as calculate magnetic scanning signals and spectral lines; and in Section 4 we draw magnetic and frequency scanning spectra for a weak probe field.

2. Velocity distribution

In the absence of electromagnetic waves, the population of a quantum system is concentrated at the lower level and depends on the velocity of particles:

$$\rho_1^{\Lambda}(v) = \rho_2^{\Lambda}(v) = F(v)/2;\ \ \rho_3^{\Lambda} = 0,$$

$$\rho_1^{\mathrm{V}}(v) = F(v);\ \ \rho_2^{\mathrm{V}} = \rho_3^{\mathrm{V}} = 0.$$

As particles interact with the traveling electromagnetic wave, some of them, due to the Doppler effect, fall in the exact resonance with the wave, that is, the following condition

$$\delta_{j\pm} = 0\ ,\ \ j = 1, 2, \qquad (7)$$

fulfills for them. Such particles are resonantly excited as a result of the interaction; the corresponding dips arise against the background of the Maxwell distribution for the lower levels, and the upper-level populations are nonzero only near the resonance, whose amplitude is proportional to $F(v)$. At a zero split or exact resonance of one of the transitions in the system, the number of resonances decreases down to three, two, or one according to degeneration of condition (7). At linear excitation (we take into account only the first order in terms of the wave intensity), the upper-level population of the Λ- and V-systems can be represented as a sum of four Lorentz profiles $L^{kv}(x, \Gamma) = \Gamma^2/[\Gamma^2 + (kv - x)]^2$, centered at the velocity x/k ($k+ = k- = k$):

$$\mathrm{P}^{\Lambda} = 2A\rho_3^{\Lambda} \cong s''; \ \ \mathrm{P}^{\mathrm{V}} = A\big(\rho_2^{\mathrm{V}} + \rho_3^{\mathrm{V}}\big) \cong 2s'',$$

$$\Gamma s'' = W_-\Big[L^{kv}(-\Omega_- - \Delta, \Gamma) + L^{kv}(-\Omega_- + \Delta, \Gamma)\Big] +$$

$$+W_+\Big[L^{kv}(\Omega_+ + \Delta, \Gamma) + L^{kv}(\Omega_+ - \Delta, \Gamma)\Big].$$

The upper-level population and, correspondingly, the total work of the field in the V-system are twice as high as those of the Λ-system, since the common normalization condition of the density matrix (6) includes the split levels with the double weight. Thus, at the low intensity of the traveling waves, the upper-level velocity distribution of the Λ- and V-systems consists of four peaks (Figs. 1*a* and *c*).

Consideration of the second order of smallness in terms of the wave intensity yields the products of the Lorentz and dispersion profiles with different centers but equal half-widths, which can be reduced to the sum of the Lorentz and Doppler profiles with different amplitudes:

$$\mathrm{P}^{\Lambda} \cong \Phi(2\gamma);\ \ \mathrm{P}^{\mathrm{V}} \cong \Phi(A + 2\gamma);$$

$$\Phi(x) = s'' - \frac{3s''^2}{2A} + \frac{\big(s'^2 - s''^2\big)\Gamma_3 + s's''4\Delta}{\big(\Gamma_3^2 + 4\Delta^2\big)} - \frac{d''^2}{x}, \qquad (8)$$

where $d = \zeta_{1-} + \zeta_{1+} - \zeta_{2-} - \zeta_{2+}$ and the prime denotes real parts of complex parameters s, d, while the double prime denotes their imaginary parts [ζ and s are determined in Eq. (3)]. The sums of the dispersion profiles correspond to the real parts, while the sums of the Lorentz profiles correspond to the imaginary parts. The sum of the Lorentz and dispersion profiles with the same centers and widths yields the shift of the peak of the resulting profile and the asymmetric shape of its wings. Thus, the wave intensity increase leads to the field broadening of some profiles and to formation of a wide nonlinear peak on the Doppler signal (Figs. 1*a* and *c*).

Under the saturation conditions, the upper-level population $\rho_{3\,\mathrm{sat}}(v)$ depends only on the relaxation constants:

$$\rho_{3\,\mathrm{sat}}(v) = F(v)/(3 + 2A/\Gamma_3)\,.$$

If the detunings from the resonance are small ($\Delta, \Omega < \Gamma$), then at linear excitation, too, the individual lines form one common profile (Figs. 1*b* and *d*), whose amplitude is maximal in the range of the medium fields. A similar, in the intensity, resonance is also observed in the case of one traveling wave interacting with a three-level system. The increase of the wave intensity leads to a decrease of the profile's peak amplitude and its broadening, and there arises a dip at the center of the profile in the case of a standing wave. If the intensities differ by more than one third, the dip is absent. The increase of the standing wave intensity leads to excitation of particles with higher velocities. This effect is limited by the Doppler profile.

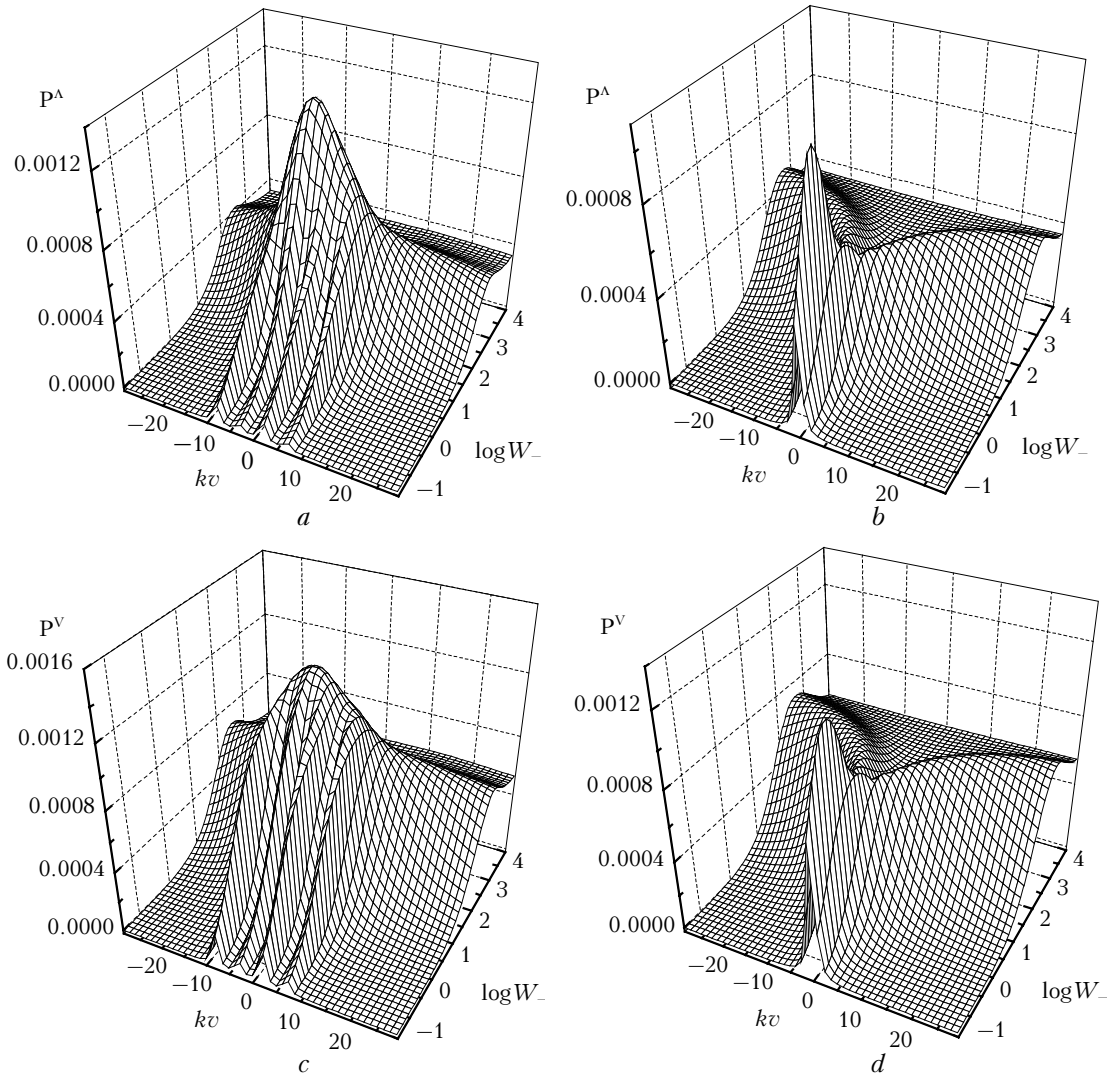

Fig. 1. Velocity distribution of upper-level population of Λ- (*a*, *b*) and V- (*c*, *d*) systems depending on the traveling wave intensity at $A = 1/2$, $\gamma = 0.1$, $\Gamma_3 = \gamma$, $\Gamma = A/2 + \gamma$, $kv = 130$ and $W_+ = W_-/3$, $\Delta = 5$, $\Omega_- = 3$, $\Omega_+ = 2$ (*a*, *c*); $W_+ = W_-$, $\Delta = 0.5$, $\Omega_- = 0.3$, $\Omega_+ = 0.2$ (*b*, *d*).

The interference shift of the resonant frequency for a stationary quantum system was considered in Ref. 1 and called the giant interference shift. In the case of one traveling wave and zero broadening coefficients, the analytical equations for $\rho_3^{\Lambda}(0)$ from Eq. (2) coincide with the results of Ref. 1.

For the case of the exact resonance of the standing wave ($W_- = W_+ = W$, $\Omega_\pm = 0$), equations (4) and (6) for the work of $P(v)$ can be reduced to a sum of the conditionally Lorentz and conditionally dispersion profiles relative to the square particle velocities:

$$P^{\Lambda, V}(v) = \frac{F(v)a_L^{\Lambda}}{\left(k^2v^2 - \Omega_{\Lambda V}^2\right)^2 + \Gamma_{\Lambda, V}^4} + \frac{F(v)a_D^{\Lambda}k^2v^2}{\left(k^2v^2 - \Omega_{\Lambda V}^2\right)^2 + \Gamma_{\Lambda, V}^4}, \tag{9}$$

where

$$a_L^{\Lambda} = 4W\left(\Gamma^2 + \Delta^2\right)\left(\Gamma + \frac{4\ \ W\ \ \Gamma_3}{\Gamma_3^2 + 4\ \ \Delta^2}\right);\ \ a_L^V = 2a_L^{\Lambda};$$

$$a_D^{\Lambda} = \frac{4W\Gamma}{A};\ \ a_D^{\Lambda} = 2a_D^{\Lambda};$$

$$\Omega_{\Lambda V}^2 = \Delta^2 - \Gamma^2 - 2W\left(1 + \frac{3\Gamma}{2A} + \frac{(2\Gamma - \Gamma_3)\Gamma_3}{\Gamma_3^2 + 4\Delta^2}\right);$$

$$\Gamma_{\Lambda}^4 = 4\Delta^2\left(2\Gamma + \frac{3W}{A}\right)\left(\Gamma - \frac{2W(2\Gamma - \Gamma_3)}{\Gamma_3^2 + 4\Delta^2}\right) +$$

$$+W^2\left(\frac{16\ \ (2\Gamma - \Gamma_3)^2\Delta^2}{\left(\Gamma_3^2 + 4\Delta^2\right)^2} - \frac{9\Gamma^2}{A^2}\right) - 4\Gamma^2\Delta^2\ ;$$

$$\Gamma_V^4 = 4\Delta^2\left(\Gamma + \frac{3W}{A}\right)\left(\Gamma - \frac{4W(2\Gamma - \Gamma_3)}{\Gamma_3^2 + 4\Delta^2}\right) +$$

$$+W^2\left(\frac{16(2\Gamma-\Gamma_3)^2\Delta^2}{\left(\Gamma_3^2+4\Delta^2\right)^2}-\frac{36\Gamma^2}{A^2}\right)+\frac{12W\Gamma\Delta^2}{A}.$$

The parameters $\Gamma^4_{\Lambda,V}$ and $\Omega^2_{\Lambda,V}$ can have both positive and negative values, but $\Omega^4_{\Lambda V} > \Gamma^4_{\Lambda,V}$ and the denominator in Eq. (9) is always positive. The obtained equation is in a full agreement with the results of numerical solution depicted in Figs. 1*b* and *d*.

The first term in Eq. (9) is the profile with the amplitude $F(0)a_L/(\Omega^4_{\Lambda V}+\Gamma^4_{\Lambda,V})$ and half-width $k^2v^2_{1/2}=\sqrt{2\Omega^4_{\Lambda V}+\Gamma^4_{\Lambda,V}}-\Omega^2_{\Lambda V}$. The second term has a zero minimum at the center and two maxima at the points $\pm\sqrt[4]{\Omega^4_{\Lambda V}+\Gamma^4_{\Lambda,V}}/k$ with the amplitude $F(0)a_D\Big/\left[2\left(\sqrt{\Omega^4_{\Lambda V}+\Gamma^4_{\Lambda,V}}+\Omega^2_{\Lambda V}\right)\right]$. The resulting distribution has a dip at the center and two side maxima with equal amplitudes:

$$2\Gamma^4_{\Lambda,V}a_{\max}=a_D\Omega^2_{\Lambda V}+a_L^{\Lambda,V}+\sqrt{\left(\Omega^2_{\Lambda V}+\frac{a_L^{\Lambda,V}}{a_D^{\Lambda,V}}\right)^2+\Gamma^4_{\Lambda,V}};$$

$$k^2v^2_{\max}=\sqrt{\left(\Omega^2_{\Lambda V}+\frac{a_L^{\Lambda,V}}{a_D^{\Lambda,V}}\right)^2+\Gamma^4_{\Lambda,V}}-\frac{a_L^{\Lambda,V}}{a_D^{\Lambda,V}}.$$

At a low intensity of the standing wave, the central dip width is determined by the split Δ and the width of the transitions Γ (the dip in Figs. 1*b* and *d* is absent, since $\Delta < 2\Gamma$). In the range of strong fields, the dip width linearly depends on the intensity, i.e., the maxima in the plots scatter exponentially with the log W increase.

Determine the standing wave intensity, at which the upper-level population is maximal, and calculate the total work at the point found:

$$4W_{\max}(v)=$$

$$=\frac{\Gamma\left(\Gamma_3^2+4\Delta^2\right)\left(\Gamma^2+\Delta^2+k^2v^2\right)}{\dfrac{Z\,\Delta\sqrt{\Gamma^2+\Delta^2}}{\sqrt{\left(\Gamma^2+\Delta^2\right)^2+2\left(\Gamma^2-\Delta^2\right)k^2v^2+k^4v^4}}-\Gamma_3\left(\Gamma^2+\Delta^2\right)};$$

$$\mathrm{P}^{\Lambda}(W_{\max})=\frac{2AF(v)}{3-2\theta},\quad \mathrm{P}^{V}(W_{\max})=\frac{2AF(v)}{3-\theta},$$

where

$$\theta=\frac{2A\Delta}{\Gamma^2}\,\frac{Z\left[\Delta\left(\Gamma^2+\Delta^2-k^2v^2\right)-\sqrt{u}\right]}{\left(\Gamma_3^2+4\Delta^2\right)\left(\Gamma^2+\Delta^2+k^2v^2\right)^2};$$

$$u=\left(\Gamma^2+(\Delta-kv)^2\right)\left(\Gamma^2+(\Delta+kv)^2\right)\left(\Gamma^2+\Delta^2\right);$$

$$Z=\left[(2\Gamma+\Gamma_3)\left(\Gamma^2+\Delta^2\right)+(2\Gamma-\Gamma_3)k^2v^2\right].$$

Since θ is proportional to Δ, as the split between the levels vanishes, the maximal upper-level populations depend only on the particle velocity $\rho_j \equiv F(v)/3$.

The field broadening of the velocity distribution of the populations at $W > 1$ becomes significant: the half-width of one line becomes comparable with the half-width of the Doppler profile, which should be taken into account when choosing a method for integration over velocities in the region of strong fields.

3. Spectrum of resonant fluorescence and magnetic scanning signal

When summing signals from different particles of the ensemble, individual spectral lines form a nonuniformly broadened Doppler profile. The magnetic scanning signal also has the Doppler shape and the characteristic dip at the zero magnetic field. Against the background of a wide spectral profile and the characteristic profile of magnetic scanning, we can separate some features: nonlinear resonances, whose positions, amplitudes, and half-widths are determined by the system parameters, magnetic field and traveling wave intensity and frequency.

Integrate Eq. (8) assuming that the width of every line is much smaller than the root-mean-square velocity of the particles in the ensemble and find the approximate equation for integral (2), separating some dimensionless Lorentz $L(x,y) = 1/(1 + x^2/y^2)$ and dispersion $D(x,y) = x/y/(1 + x^2/y^2)$ profiles against the background of wide Doppler profiles

$$\exp\left(-\Delta^2/\overline{v}^2\right)\cong\exp\left(-\Omega_0^2/\overline{v}^2\right)\cong\exp\left[-(\Delta\pm\Omega_0)^2/\overline{v}^2\right]\cong 1:$$

$$\frac{k\overline{v}}{\sqrt{\pi}}\left(\mathrm{P}^{\Lambda}-\mathrm{P}_1^{\Lambda}\right)=\frac{A-3\gamma}{4A\Gamma\gamma}X1-\frac{A+3\gamma}{4A\Gamma\gamma}X2+$$

$$+\frac{L(2\Delta,\Gamma_3)}{\Gamma\Gamma_3}X3+\frac{D(2\Delta,\Gamma_3)}{\Gamma\Gamma_3}X4;$$

$$\frac{k\overline{v}}{4\sqrt{\pi}}\left(\mathrm{P}^{V}-\mathrm{P}_1^{V}\right)=\frac{-A-3\gamma}{A\ \ (A+2\gamma)\Gamma}X1-\frac{2A+3\gamma}{A(A+2\gamma)\Gamma}X2+ \qquad (10)$$

$$+\frac{L(2\Delta,\Gamma_3)}{\Gamma\Gamma_3}X3+\frac{D(2\Delta,\Gamma_3)}{\Gamma\Gamma_3}X4,$$

where

$$X1=(W_-^2+W_+^2)L(\Delta,\Gamma)+2W_-W_+L(\Omega_-+\Omega_+,\Gamma);$$

$$X2=W_-W_+[L(2\Delta-\Omega_--\Omega_+,2\Gamma)+L(2\Delta+\Omega_-+\Omega_+,2\Gamma)];$$

$$X3=(W_-^2+W_+^2)L(\Delta,\Gamma)+W_-W_+[L(2\Delta-\Omega_--\Omega_+,2\Gamma)+$$

$$+L(2\Delta+\Omega_-+\Omega_+,2\Gamma)];$$

$$X4=(W_-^2+W_+^2)D()+W_-W_+[D(2\Delta-\Omega_--\Omega_+,2\Gamma)+$$

$$+D(2\Delta+\Omega_-+\Omega_+,2\Gamma)].$$

Equation (10) describes nonlinear resonances standing out against the background of the Doppler

profile in the region of weak fields. Obviously, resonances with the positions depending only on Δ are realized at magnetic scanning, and resonances with the position depending only on $\Omega_{\pm}$ are realized at frequency scanning. Resonances depending on frequency detunings and on the split magnitude are observed in the both versions of the experiment, and their positions are determined respectively by the magnetic field or by the frequencies of the traveling waves. The resonances in the Λ- and V-systems have the same positions and half-widths, but their amplitudes differ significantly only at small γ. In the case of V-system, the terms with $X1$ and $X2$ describe nonlinear dips, whose amplitude is inversely proportional to $A + \gamma$. For the case of Λ-system, the first two terms in Eq. (10) are inversely proportional to the broadening coefficient γ, and the first term alternates the sign at $\gamma = A/3$. At γ, $\Gamma_3 \to 0$ the approximation of low intensities in form (10) is incorrect, but exact equations (2) and (4) for small γ and Γ_3 cannot be integrated analytically, therefore the limiting case will be treated numerically. Figure 2 depicts the pressure dependence of the magnetic and frequency scanning signals for Λ-systems at the standing wave intensity $W = 0.1$ (Figs. 2*a* and *c*) and the corresponding intensity dependence at $\gamma = 0.01$ (Figs. 2*b* and *d*) obtained through numerical solving and integrating of the problem. Compare the features of the drawn profiles with the resonances separated in Eq. (10).

The plot of the frequency scanning signal (Fig. 2*c*) has three resonances in the region of low pressure. The central peak at $\Omega = 0$ transforms into a dip with the increasing pressure, as follows from Eq. (10). At zero pressure this resonance increases up to a finite quantity, and the side dips described in the second term of Eq. (10) are almost invisible in the plot.

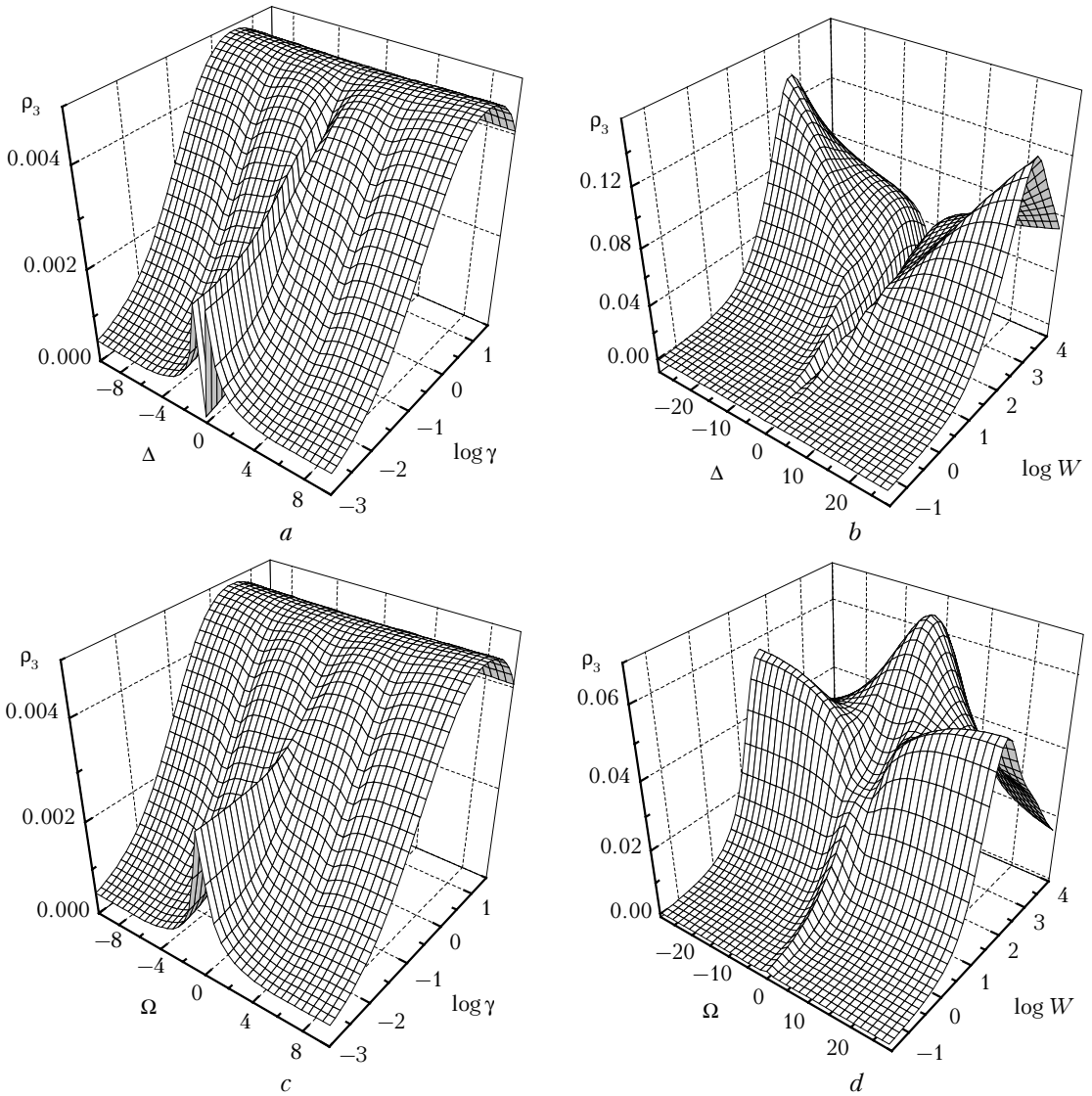

Fig. 2. Magnetic scanning signal (*a*, *b*) and line profile (*c*, *d*) vs. pressure (*a*, *c*) and standing wave intensity (*b*, *d*) at $A = 1/2$, $\Gamma_3 = \gamma$, $\Gamma = A/2 + \gamma$, $k\overline{v} = 130$, $\Omega_{\pm} = 5$ (*a*, *b*) and $\Delta = 5$ (*c*, *d*), and $W_{\pm}$=0.1 (*a*, *c*) $\gamma = 0.01$ (*b*, *d*).

The magnetic scanning signal has a more complex shape (Fig. 1*a*). At a zero split, the first and third terms in Eq. (10) are maximal. The first term corresponds to the peak at low pressure, while the third one corresponds to the dip. With the increase of γ the amplitudes of the resonances decrease. An increase of the standing wave intensity (Figs. 1*b* and *d*) leads to the increase of the Doppler signal amplitude and to transformation of the resonances; in this process, the central resonance on the line profile twice alternates its sign.

Integrate Eq. (9) using the theory of residues. Thus we obtain the work proportional to the upper-level population of the Λ- and V-systems at zero detuning of the standing wave:

$$2\sqrt{\pi}k\bar{v}\mathrm{P}^{\Lambda,\mathrm{V}} = \mathrm{Re}\left[\frac{\exp(Z_-^2/k^2\bar{v}^2)}{\pm\Gamma_{\Lambda,\mathrm{V}}^2}\left(\frac{a_L^{\Lambda,\mathrm{V}}}{Z_-} - a_D^{\Lambda,\mathrm{V}}Z_-\right) - \frac{\exp(Z_+^2/k^2\bar{v}^2)}{\Gamma_{\Lambda,\mathrm{V}}^2}\left(\frac{a_L^{\Lambda,\mathrm{V}}}{Z_+} - a_D^{\Lambda,\mathrm{V}}Z_+\right)\right], \qquad (11)$$

$$Z_\pm^2 = \Omega_{\Lambda\mathrm{V}}^2 \pm i\Gamma_{\Lambda,\mathrm{V}}^2.$$

In the first term's denominator of Eq. (11) we take "+" at $\Gamma_{\Lambda,\mathrm{V}}^4 > 0$ or "−" at $\Gamma_{\Lambda,\mathrm{V}}^4 < 0$, and at $\Gamma_{\Lambda,\mathrm{V}}^4 = 0$ the total work of the fields is

$$\left(\frac{a_L^{\Lambda,\mathrm{V}}}{2\Omega_{\Lambda V}^2} - \frac{a_L^{\Lambda,\mathrm{V}}}{k^2\bar{v}^2} + \frac{a_D^{\Lambda,\mathrm{V}}}{2} + \frac{a_D^{\Lambda,\mathrm{V}}}{k^2\bar{v}^2}\right)\exp\frac{\Omega_{\Lambda\mathrm{V}}^2}{k^2\bar{v}^2} \Big/ \left(\sqrt{\pi}k\bar{v}\Omega_{\Lambda\mathrm{V}}\right).$$

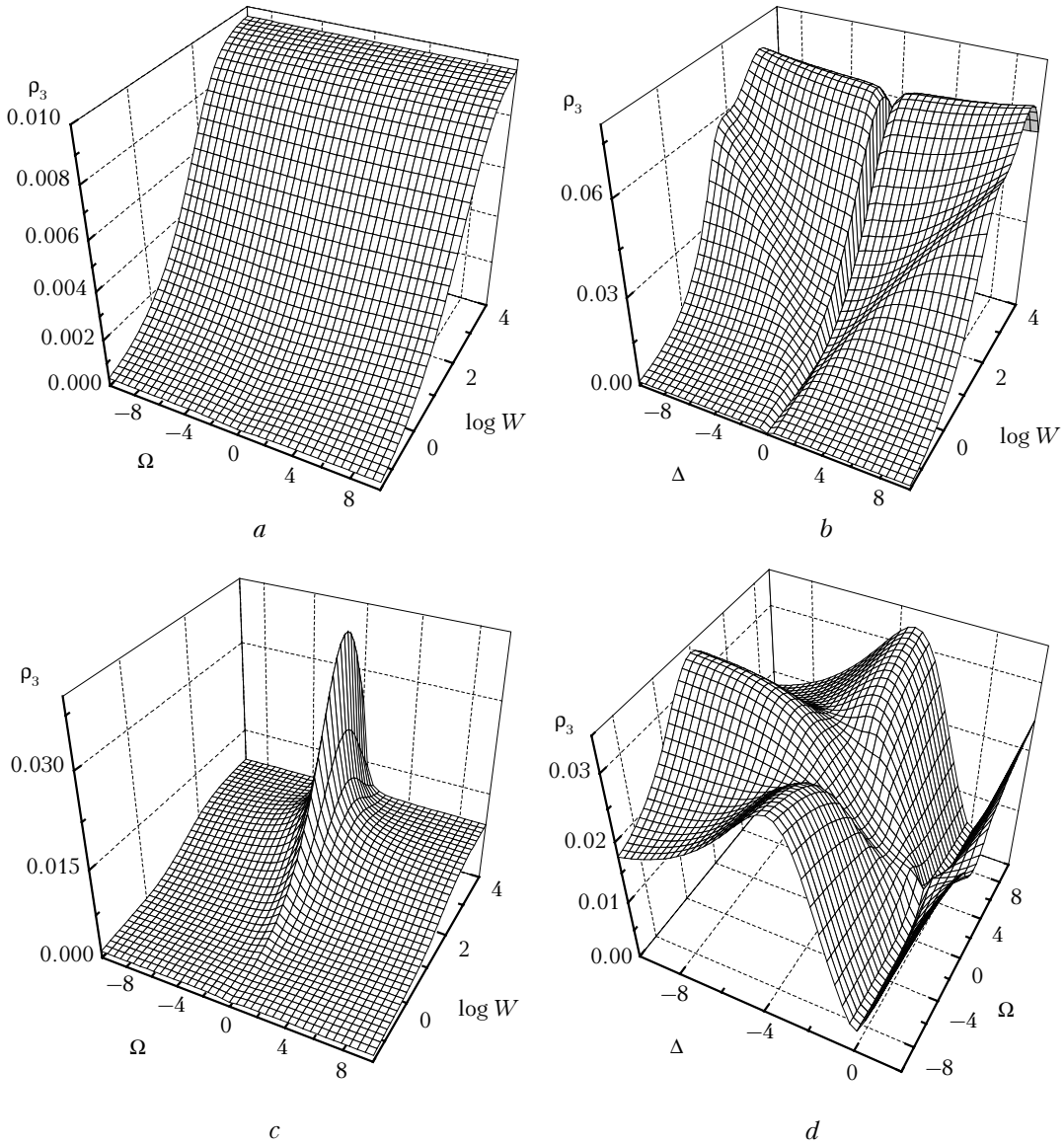

Fig. 3. Line profile (*a*, *c*) and magnetic scanning signal (*b*) vs. standing wave intensity and upper-level population vs. split and detuning from resonance (*d*) at $A = 1/2$, $\Gamma_3 = \gamma$, $\Gamma = A/2 + \gamma$, $\gamma = 0.01$, $k\bar{v} = 130$ and $\Delta = 0$ (*a*), $\Omega_\pm = 0$ (*b*), $\Delta = 0.1$ (*c*), $W = 10$ (*d*).

Equation (11) for extremes in Δ and W can be obtained numerically.

The plots of the line profile at the zero split and the magnetic scanning signal at the exact resonance are shown in Figs. 3*a* and *b* at different values of the standing wave intensity. The line profile has no features and demonstrates only uniform intensification with following saturation. In this case, Doppler broadening levels off the nonlinear effects. In the magnetic scanning signal described by Eq. (11), one dip broadens at the zero split with the increasing field (similarly to the case of excitation by one traveling wave), while another one has a constant width.

The small increase of the split significantly changes the frequency scanning signals (Fig. 3*c*): the nonlinear resonance with the amplitude twice as high as that of the Doppler signal arises in the region of medium fields. It should be noted that the maximum population in this plot is roughly halved as compared to the maximum population at $\Delta = 5$ (see Fig. 2*d*). The shape of the magnetic scanning signal is not changed at small detuning of the standing wave from the resonance.

Figure 3*d* depicts the dependence of the upper-level population of the Λ-system on the frequency detuning from the resonance and on the split magnitude at the standing wave intensity $W = 10$. This plot allows us to evaluate the dependence of the line profile on the split magnitude and the dependence of the magnetic scanning signal on the detuning. At variation of the split magnitude, the shape of the line profile changes significantly, namely, at $\Delta = 1$–8 a dip is observed at the center of the profile in contrast to the peak at all other values of Δ. The dip in the magnetic scanning signal becomes narrower in the region of zero detuning.

4. Pump-probe technique

Assuming that the wave intensity W_- is much lower than W_+, let us study the spectra of frequency and magnetic scanning of a weak probe wave. In the second approximation in terms of intensity, separate nonlinear resonances in the work of the field of one wave:

$$\frac{k\bar{v}\sqrt{\pi}\left(\mathrm{P}_{-}^{\Lambda}-\mathrm{P}_{1-}^{\Lambda}\right)}{\sqrt{\pi}\,W_{+}W_{-}}=\frac{A-3\gamma}{2A\Gamma\gamma}Y1-$$

$$-\left[\frac{A+3\gamma}{4A\Gamma\gamma}+\frac{L(2\Delta,\Gamma_3)}{\Gamma\Gamma_3}\right]Y2+\frac{D(2\Delta,\Gamma_3)}{\Gamma\Gamma_3}Y3;$$

$$\frac{k\bar{v}\left(\mathrm{P}_{-}^{\mathrm{V}}-\mathrm{P}_{1-}^{\mathrm{V}}\right)}{\sqrt{\pi}2W_{+}W_{-}}=-\frac{2(A+3\gamma)}{A(A+2\gamma)\Gamma}Y1- \tag{12}$$

$$-\left[\frac{2A+3\gamma}{A(A+2\gamma)\Gamma}+\frac{L(2\Delta,\Gamma_3)}{\Gamma\Gamma_3}\right]Y2+\frac{D(2\Delta,\Gamma_3)}{\Gamma\Gamma_3}Y3,$$

where

$$Y1 = L(\Omega_- + \Omega_+,\Gamma);$$

$$Y2 = L(2\Delta - \Omega_- - \Omega_+,2\Gamma) + L(2\Delta + \Omega_- + \Omega_+,2\Gamma);$$

$$Y3 = D(2\Delta - \Omega_- - \Omega_+,2\Gamma) + D(2\Delta + \Omega_- + \Omega_+,2\Gamma).$$

All the resonances separated depend on the product of intensities of the two waves. The resonance of the first term in Eq. (12) is centered at the frequency of zero detuning, and for the Λ-system it alternates the sign with the increasing pressure. The resonances of the second term ($Y2$) are maximal when the traveling wave frequency coincides with the frequencies of allowed transitions 1 and 2. The third term in Eq. (12) is proportional to the product of the dispersion profiles with different positions and half-widths.

Figure 4 depicts the plots of the probe field work for Λ- and V-systems at the exact resonance of the pump wave ($\Omega_+ = 0$). The calculation conditions correspond to the situation that the first term is positive for the Λ-system and negative for the V-system. In the plots corresponding to frequency scanning of the Λ-system (Fig. 4*a*), we can see the peak ($\Omega = 0$) and two side dips ($\Omega = \pm 5$), while for the V-system we see three dips at the same points (Fig. 4*c*). The side resonances correspond to the sum of the Lorentz profiles $Y2$. The same resonances on the plots corresponding to magnetic scanning ($\Delta = \pm 5$, Figs. 4*b* and *d*) fall on the dip of zero split.

Note that in the region of nonlinear interaction of the probe wave and the counterrunning pump wave, the increase in the intensity of the latter leads to decrease in the work of the probe field. The plots in Fig. 4 at $W > 100$ include zones, in which the work of the probe field is negative, that is, the probe wave is intensified.

Conclusion

The use of the standing wave or two traveling counterrunning waves of the same frequency and close intensity for resonance excitation of atoms allows us to obtain a dip at a zero magnetic field; the dip's width is determined by the gas pressure in the cell and independent of the pump power. The increase of the pump radiation detuning from the resonance leads to the signal amplitude decrease.

Nonlinear interference effects are suppressed by chaotic motion of gas atoms and molecules. Therefore, to distinguish nonlinear resonances against the background of the Doppler profile, the biharmonic excitation by, for instance, backward traveling waves is needed. In this case, the profile of the resonant fluorescence line is more sensitive to the radiation and atom parameters than the magnetic scanning signal.

The interaction of gas atoms in the magnetic field with backward traveling modes, considered theoretically in this paper, can find its practical application in spectroscopy of nonlinear resonances and physics of gas lasers tuned by the magnetic field. The needed conditions are: gas pressure of 1–5 Torr, radiation intensity of 0.5–5 W/cm^2, and the magnetic field strength of 0–20 G. Particular attention should be paid to the effect of sign alternation of the nonlinear resonance with increasing pressure for systems with a split ground state, since this effect can be used in solving the inverse spectroscopic problem.

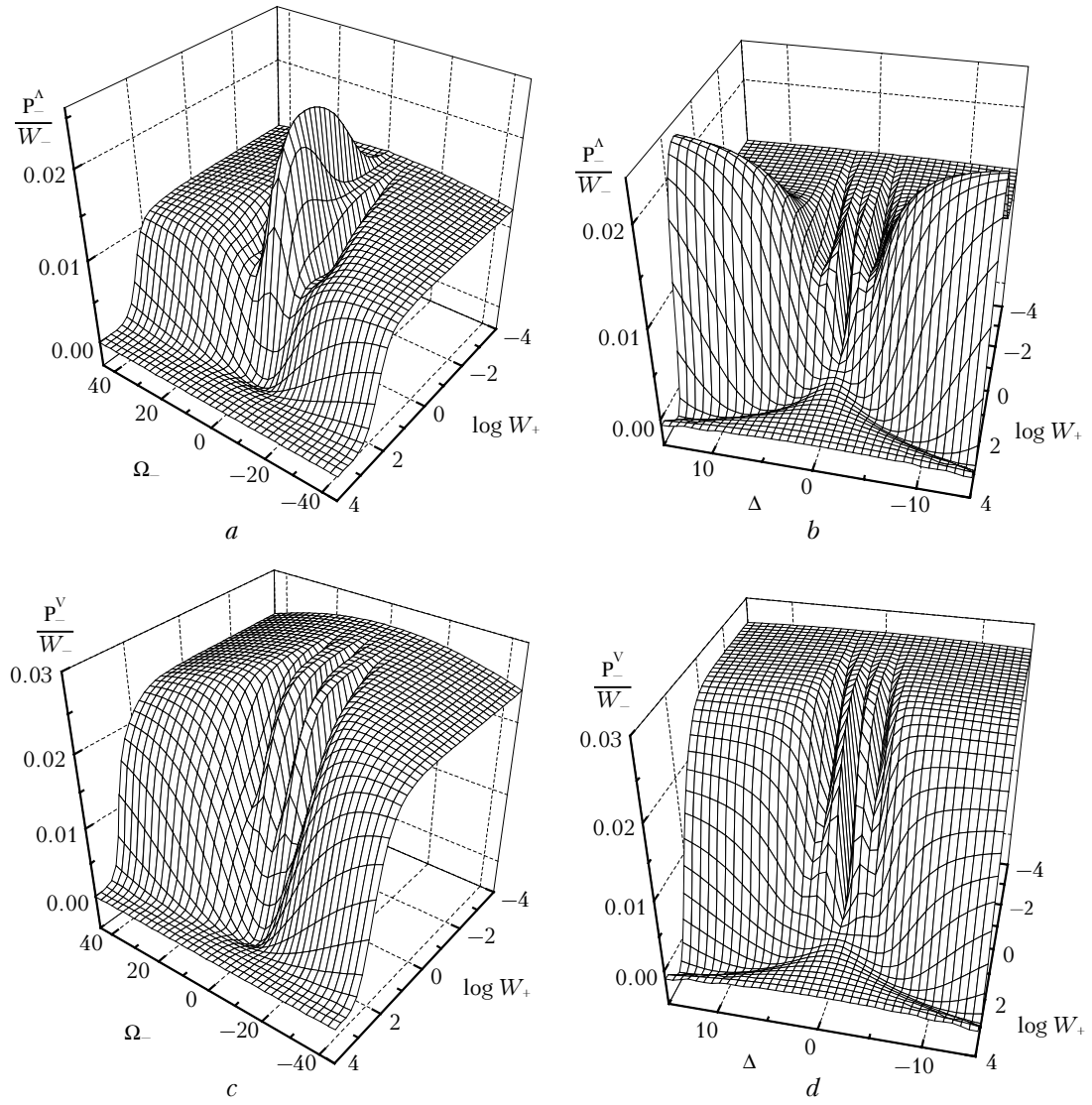

Fig. 4. Work of the probe field vs. the detuning frequency (*a*, *c*) and the split value (*b*, *d*) at different intensity of the pump wave and at $A = 1/2$, $\Gamma_3 = \gamma$, $\Gamma = A/2 + \gamma$, $\gamma = 0.01$, $W_- = 10^{-7}$, $\Omega_+ = 0$, $k\overline{v} = 130$ and $\Delta = 5$ (*a*, *c*), $\Omega_- = 5$ (*b*, *d*).

References

1. M.S. Zubova and V.P. Kochanov, Zh. Eksp. Teor. Fiz. **101**, No. 6, 1772–1786 (1992).
2. B.D. Agapov, M.B. Gornyi, and B.G. Matisov, Usp. Fiz. Nauk **163**, No. 9, 1–36 (1993).
3. M.P. Chaika, *Interference of Degenerate Atomic States (Overlapping of Levels)* (Leningrad State University Press, Leningrad, 1975), 192 pp.
4. N.G. Lukomskii, V.A. Polishchuk, M.P. Chaika, and E.A. Alipieva, Opt. Spektrosk. **83**, No. 3, 420–426 (1997).
5. V.S. Letokhov and V.P. Chebotaev, *Principles of Nonlinear Laser Spectroscopy* (Nauka, Moscow, 1975), 280 pp.
6. I.A. Kartashov and A.V. Shishaev, Pis'ma Zh. Eksp. Teor. Fiz. **58**, No. 7, 501–504 (1993).
7. S.G. Rautian, G.I. Smirnov, and A.M. Shalagin, *Nonlinear Resonances in Atomic and Molecular Spectra* (Nauka, Novosibirsk, 1979), 312 pp.